Northumbria Research Link

This version was downloaded from Northumbria Research Link: http://nrl.northumbria.ac.uk/28778/

www.northumbria.ac.uk/nrl

northumbria
UNIVERSITY NEWCASTLE

Investigation on iterative multiuser detection physical layer network coding in two-way relay free-space optical links with turbulences and pointing errors

ZINA ABU-ALMAALIE,[1, *] ZABIH GHASSEMLOOY, [1] MANAV R. BHATNAGAR,[2] HOA LE-MINH,[1] NAUMAN ASLAM,[3] SHIEN-KUEI LIAW,[4] AND IT EE LEE [5]

[1]Optical Communications Research Group, Faculty of Engineering and Environment, Northumbria University, Newcastle Upon Tyne, UK
[2]Department of Electrical Engineering Indian Institute of Technology-Delhi, New Delhi, India
[3]Computational Intelligence Research Group, Faculty of Engineering and Environment, Northumbria University, Newcastle Upon Tyne, UK
[4]Department of Electronic and Computer Engineering National Taiwan University of Science and Technology, Taipei 106, Taiwan
[5]Faculty of Engineering, Multimedia University, 63100 Cyberjaya, Malaysia
*Corresponding author: zina.almaalie@northumbria.ac.uk

Physical layer network coding (PNC) improves the throughput in wireless networks by enabling two nodes to exchange information using a minimum number of time slots. The PNC technique is proposed for two-way relay channel free space optical (TWR-FSO) communications with the aim of maximizing the utilization of network resources. The multipair TWR-FSO is considered in this paper, where a single antenna on each pair seeks to communicate via a common receiver aperture at the relay. Therefore, chip-interleaving is adopted as a technique to separate the different transmitted signals at the relay node to perform PNC mapping. Accordingly, this scheme relies on the iterative multiuser technique for detection of users at the receiver. The bit error rate (BER) performance of the proposed system is examined under the combined influences of atmospheric loss, turbulence-induced channel fading and the pointing errors (PEs). By adopting the joint PNC mapping with interleaving and multiuser detection techniques, the BER results show that the proposed scheme can achieve a significant performance improvement against the degrading effects of turbulences and PEs. It is also demonstrated that a larger number of simultaneous users can be supported with this new scheme in establishing a communication link between multiple pairs of nodes in two time slots, thereby improving the channel capacity.

1. INTRODUCTION

Free space optical (FSO) communications is a promising complementary alternative over the conventional radio frequency (RF) technology, which has attracted attention within the research community due to their secure transmission, large bandwidth, small component sizes with low cost, and immunity to the electromagnetic interference [1]. However, optical signal propagation in free space is significantly affected by the atmospheric channel conditions such as the turbulence and pointing errors (PEs), thereby increasing the bit error rate (BER) and severely degrading the overall link performance. For a link range from a few meters to longer than 1 km, turbulence-induced signal fading becomes a major performance limiting factor in FSO systems. To combat such fading effect and maintain acceptable performance levels, several mitigation techniques have been proposed for FSO systems, which include the forward error correction (FEC), spatial diversity techniques, and cooperative diversity. Recently, research in FSO has focused on performance evaluation of multihop communication systems under the atmospheric turbulence condition, where the source node communicates with the destination node via a number of relay nodes (RNs) in a serial configuration. Multihop transmission is a promising technique to achieve broader coverage and mitigate wireless channels impairment, and it has a number of advantages including increased capacity, avoiding the use of cables, low cost and minimizing the need for a fixed infrastructure [2-4]. In particular, the relay-assisted FSO system has drawn significant attention as an efficient technique to extend the coverage area and improve the system performance in the presence of non-line-of-sight path between two FSO nodes in the network [5,6]. Thus, the relay-assisted FSO transmission can take advantage of the resulting shorter and multiple-hop links between the transmitter

(Tx) and the receiver (Rx) in order to improve the system performance and increase the link reliability.

In recent year, network coding (NC) has been introduced in wireless networks to establish a new form of cooperative relay technology, mainly due to its capability to increase the system throughput and combat link failures by distributing the traffic over a larger number of communication paths [7]. NC allows intermediate network nodes to perform arbitrary mathematical operations to combine the data received from different links, thus offering numerous advantages over the traditional routing schemes [8]. This has been extensively studied in the context of optical multicast networks [9,10]. To mitigate the strong turbulence-induced fading, a cooperative relaying aided FSO transmission network based on NC and using an iterative multiple source detection scheme in conjunction with a chip-level soft network decoding at the relay and the destination node was proposed in [11]. The simulation results demonstrated that the proposed method was capable of approaching the single user bound for transmission over the gamma–gamma turbulence channel. Additionally, this technology has been adopted as a widely accepted solution for combatting turbulence-induced fading in two-way relay channel (TWRC) FSO systems [12-14]. Furthermore, the concept of NC can also be applied to the physical layer that deals with signal reception and modulation, and is known as the physical layer NC (PNC) [15]. PNC leads to further improvement of the wireless transmission throughput through the effective use and exploitation of wireless resources. Recently, many researchers, due to the need for higher data rates and faster connection speeds in wireless networks, have adopted this technique. The PNC system was first considered for a TWRC where two users transmitted their information simultaneously with the aid of RN.

However, a substantial number of analytical and simulation studies of the two-way relay FSO (TWR-FSO) system have considered only the amplifier-and-forward (AF) and decoder-and-forward (DF) schemes or have adopted the linear NC at the RNs. Therefore, inspired by the advantage of the PNC technique, which offers a higher data rate and faster connection speed in wireless networks, it was proposed for the TWR-FSO communications where there is no direct path between the two FSO communication nodes [16]. The model was referred to as TWR-FSO PNC, where the authors explored the advantage of PNC technique for full utilization of network resources.

Despite of a significant amount of research being carried out in TWR for PNC, increasing the number of users which can simultaneously be transmitted to the RN is still considered as the main constraint in such systems. This is mainly because the PNC mapping can only support two users for exchanging their information at the same time over TWR. Therefore, very little work has been reported on the impact of increasing the number of communication pair on the performance of the PNC system assuming different strategies [17-19]. Recently, multiple access techniques referred to as interleave division multiple access (IDMA) technique was suggested in [20, 21].

In this paper, to allow multiple pairs of user to swap their data between them within a single RN over FSO link, the effectiveness of iterative multiuser (I-MUD) detection based PNC is embraced. It is assumed that the pair of users cannot receive each other's signals directly, and hence the RN is the enabler of communication. Therefore, the chip-interleaving approach for user separation, in order to perform PNC demapping at the intermediate node, is adopted. This scheme referred to as I-MUD TWR-FSO PNC, which offers a bi-directional half-duplex relaying network that consists from K user communicate with each other via a single RN, as shown in Fig. 1. The performance of the system in terms of BER is examined by considering link impairments imposed by the atmospheric attenuation because of beam extinction and channel fading caused by turbulence (ranging from weak to strong turbulence) and the PEs. The simulation results reveal the ability of the proposed scheme to establish communication between the multiple nodes with a minimum number of transmission phases, even when the number of simultaneous users is increased.

The rest of the paper is organized as follows: Section 2 describes the system model. Section 3 defines the atmospheric channel, while Section 4 describes the error rate analysis considered in this study. Next, simulation results and discussions are presented in Section 5. Finally, conclusions are drawn in Section 6.

2. SYSTEM MODEL

In an I-MUD FSO PNC model, each pair of users P exchanges their information using the RN in two transmission phases. The first phase is dedicated to the entire user transmit the information in multiple access (MA) channel to the RN. The second phase is broadcasting the RN information to the destination in broadcast channel (BC), as shown in Fig. 1. Assuming all nodes operate over a half-duplex link and full transmissions synchronization between the nodes with the same transmits power for all nodes. We assume intensity modulation with direct detection (IM/DD) for all the source nodes and the RN. Also, the noise is modelled as additive white Gaussian noise (AWGN) with zero mean and variance $\sigma^2 = N_o/2$, where $N_o/2$ is the two-sided noise power spectral density. In traditional FSO systems, on-off keying (OOK) is commonly used because of its simplicity and low-cost despite of the difficulty of adaptively adjusting the threshold. On the other hand, pulse-position modulation (PPM) signalling has excellent power efficiency with no requirement for adaptive threshold compared to OOK; however, it has poor bandwidth efficiency due to the use of shorter pulses [22]. To overcome the limitations of OOK and PPM, the binary phase shift keying (BPSK) is embraced in our proposed system. The following sub-sections outline in detail the operation of the Tx, RN and Rx for the system under consideration.

A. Transmitter

The basic Tx structure for the I-MUD TWR-FSO PNC model is shown in Fig. 2. The input binary data sequence $d_k \in (0,1)$, where $k = (1, \ldots, K)$ represents the number of users, is encoded using the convolutional encoder module (ENC) with a rate R_c. The coded bit stream $c_k \in (0,1)$ is further encoded using a simple spreading code module (SP) with a rate R_r to produce s_k. The same spreading sequence is used for all nodes. The coded sequence is then permutated by the same chip-level interleaver Π_p for each P, thus producing an interleave sequence $I_k \in (0,1)$ [23]. These interleaves can be generated independently and randomly for each P, which scrambles the error burst of the code sequence prior to the transmission. The
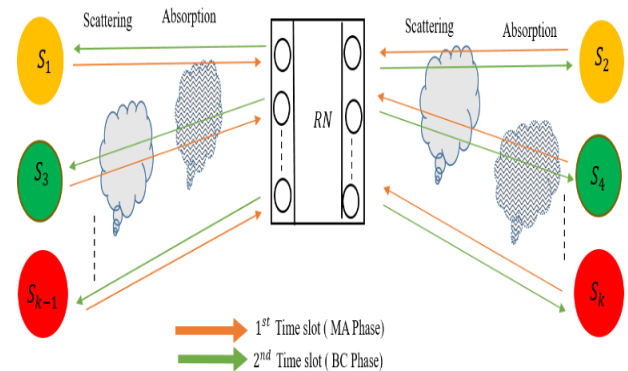

Fig. 1. Block diagram of the I-MUD TWR-FSO PNC model.

interleaver sequence is then used for modulating an RF signal using BPSK modulation, which is presented as

$$m_k = \sum g(t-T)\cos(w_c+\theta), \qquad (1)$$

where $g(t)$ is a rectangular shaping pulse function, T is bit duration, w_c is a carrier frequency, and θ is phase angular equal to 0 or π depending if a binary one or a binary zero is transmitted. To ensure the modulated signals are all positive, a direct current (DC) level bias b_o is introduced prior to IM of the light source [24]. The output optical signal at the laser diode can be expressed as

$$x_k = P_t\left[1+\zeta\, m_k\right], \qquad (2)$$

where P_t is the average transmitted optical power, and ζ is the modulation index satisfying the condition $-1 \leq \zeta\, m_k \leq 1$ to avoid clipping due to over-modulation [24].

B. Relay node

In the MA phase, all users are simultaneously transmitting to the RN, where each P swap their information using single RN. We assume that each user node is equipped with single aperture antenna directed to the corresponding aperture at RN, whereas the RN consists of two directional antennas each having K antenna aperture directed to the corresponding user's nodes. The received optical beam at the RN is detected by a photodetector (PD) with optical-to-electrical efficiency denoted by R, then is amplified using a trans-impedance amplifier (TIA) as shown in Fig. 3. The signal at the output of the PD from all users are collected and sent to the deinterleaved process. The channel state of the FSO link is modelled as a stochastic process denoted by h_k, which represents the normalized irradiance accounted for the intensity fluctuations due to the atmospheric loss, turbulence and PEs (as explained in detail later on). However, the channel coefficients are assumed to be the same for both transmissions phases. Thus, the received electrical signal for the MA phase can be represented as

$$y_r = R\sum_{k=1}^{K} h_k\, x_k + w_r, \qquad (3)$$

where h_k is the FSO channel fading coefficient from the kth users to the RN. The term w_r denotes the AWGN arising from various sources, which include the shot noise due to the signal itself, ambient light, dark current noise, and electrical thermal noise. Following down conversion, the deinterleaving procedure $\widehat{\Pi}_p$ is applied to the superimposed signal for
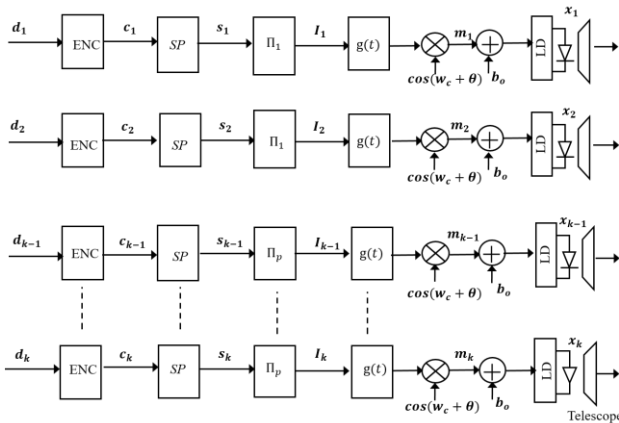
each P, which places the received code bits back in the proper order, $\hat{I}_{k-1,k}$. Through PNC demapping detection at the RN, the received signal can be mapped to the module-2 addition of the digital bit stream so that the interference becomes part of the arithmetic operation in the NC [15]. The minimum distance estimation is used to map the superimposed symbol to a network-coded symbols for each pair and, for $P = 1$, can be written as

$$x_1 \oplus x_2 = \underset{x_1,x_2\in(1,-1)}{\arg\min}\left|\hat{I}_{1,2}-\left(h_1\,x_1+h_2\,x_2\right)\right|. \qquad (4)$$

In order to successfully distinguish every network coded symbols for its target users, they are distinguished again by user specific interleave. Following BPSK modulation $\hat{x}_p^r$ and DC level bias, all signals are summed up for transmission over their corresponding FSO link [25]. A Tx telescope is used to collect, collimate, and direct the optical radiation toward the Rx telescope at the other end of the channel.
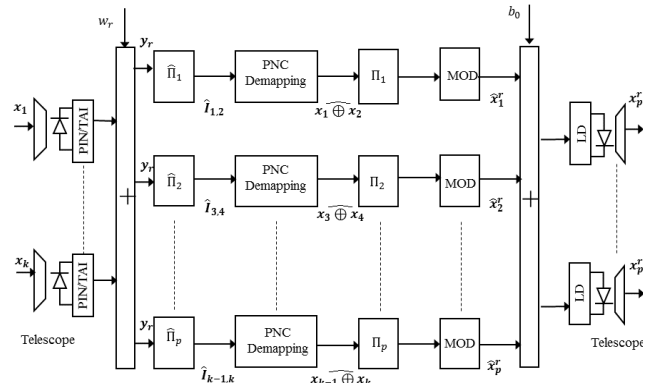
C. Receiver

The performance of the I-MUD FSO PNC model is expected to deteriorate due to MA interference (MAI) from other active users as well as the scintillation effect. Inspired by the success of the turbo code, I-MUD detection has been widely used owing to its ability to improve the system performance at a relatively low computational cost. Note that the complexity of the decoder is independent of K [23]. Therefore, the I-MUD technique is adopted to improve the system performance by eliminating the negative effect of each user on each other by iteratively exchanging the extrinsic information between the MUD and channel decoders (DECs).

The block diagram for the Rx structure is shown in Fig. 4. As in the RN, the telescope collects the incoming light and focuses it onto the PD, the output of which is amplified and processed. The electrical signal at the input to the MUD can be expressed as

$$y_{sp} = R\,P_t\,h_k\,x_p^r + w_k. \qquad (5)$$

The iterative Rx comprises of a MUD module, deinterleaver/interleaver pairs, despreader/spreading pairs and soft-in-soft-out (SISO) decoders [26]. The posteriori log-likelihood ratio (LLR) of a transmitted code bit based on the MA constraint is given by [26]

$$L_{dem}(x_p^r) = log\left[\frac{p_r(y_{sk}|x_p^r=1)}{p_r(y_{sk}|x_p^r=1)}\right], \qquad (6)$$

Fig. 2. Block diagram of the transmitter structure for the I-MUD FSO PNC model for K users at code rate $R_c = 1/2$, and spreading rate $R_r = 1/8$.

Fig. 3. Relay structure for the I-MUD TWR-FSO PNC model, which is applied PNC demapping on the received signal after a pair of user separated by their distinct chip-level interleave.

where p_r is the conditional probability distribution of the observed channel. In the case of first pairs, Equation (5) can be rewritten as

$$y_{s1} = R\,P_t h_1\,x_1^r + \sum_{\bar{p}=1,\bar{p}\neq p}^{P} h_p\,x_{\bar{p}}^r\,, \tag{7}$$

where

$$\xi_1 = \sum_{\bar{p}=1,\bar{p}\neq p}^{P} h_{\bar{p}}\,x_{\bar{p}}^r + w_k\,, \tag{8}$$

is the sum of the MAI and the noise in terms of y_{s1} relative to x_1^r. Assume that x_1^r is independent and identically distributed random variable, the conditional probability $p_r[y_{s1}|x_1^r = 1 \text{ or } 0]$ can be characterized by the Gaussian probability density function (PDF) as given by

$$p_r(y_{s1}|x_1^r = 1,0)$$
$$= \exp\left[\frac{(y_{s1}-(\pm h_1 + E(\xi_1)))^2}{2\mathrm{Var}(\xi_1)}\right]\Big/\sqrt{2\pi\,\mathrm{Var}(\xi_1)}\,, \tag{9}$$

where $E(.)$ and $\mathrm{Var}(.)$ are the total mean and variance of distortion, respectively, and can be defined as [23]

$$E(\xi_1) = \sum_{\bar{p}=1,\bar{p}\neq p}^{P} h_{\bar{p}}\,E(x_{\bar{p}}^r),$$
$$\mathrm{Var}(\xi_1) = \sum_{\bar{p}=1,\bar{p}\neq p}^{P} \left|h_{\bar{p}}\right|\mathrm{Var}(x_P^r) + \sigma^2\,. \tag{10}$$

Correspondingly, Equation (6) can be rewritten as

$$L_{dem}(x_1^r) = \log\left\{\exp\left(\frac{(y_{s1}-h_1\,R - E(\xi_1))^2}{2\mathrm{Var}(\xi_1)}\right)\right\} - \log\left\{\exp\left(\frac{(y_{s1}+h_1\,R - E(\xi_1))^2}{2\mathrm{Var}(\xi_1)}\right)\right\}$$
$$= 2\,h_1\,R\left(\frac{y_{s1}-E(\xi_1)}{Var(\xi_1)}\right). \tag{11}$$

To restore the original ordering of the sequences in the symbol, the permutation of the received signal will be deinterleaver $L_{dem}(x_1^r(\hat{I}_1))$. Prior to delivering the signal to the DECs, the signal is passed through the despreading (DSP) module. Each group of deinterleaver chips within one-bit duration is summed up by means of the despreading operation. A *posteriori* LLR for coded bits can be determined as

$$L_{desp}(c_a) = \sum_{j=1}^{s_f} \log\left[\frac{p_r(s_a(j)=1|y_{s1}(j))}{p_r(s_a(j)=0|y_{s1}(j))}\right],$$
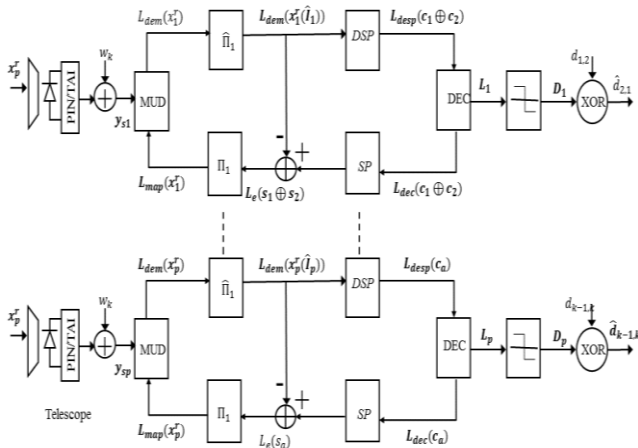

Fig. 4. Receiver structure for I-MUD TWR-FSO PNC model.

$$= \sum_{j=1}^{s_f} L_{dem}(x_1^r(\bar{I}(j)))\,, \tag{12}$$

where s_f is the spreading factor and $j = 1,..,s_f$, and c_a, s_a represent the XOR-ed coded and spreading sequence $(c_1 \oplus c_2)$, $(s_1 \oplus s_2)$, respectively. The output of the DSP module is used as *a priori* information to DECs module of the convolutional code, which performs the standard *a posteriori* probability (APP) decoding [26]. The APP algorithm is used to generate the information on the data bit stream as well as the extrinsic information on the coded bits. The final *a posteriori* LLR of the coded bits is given by:

$$L_{dec}(c_a) = \log\left[\frac{p_r(c_a=1|L_{desp}(c_a))}{p_r(c_a=0|L_{desp}(c_a))}\right]. \tag{13}$$

The output of DEC is then applied to the SP. To compute the chip-level extrinsic LLR information of the corresponding coded bits, the following equation is used:

$$L_e(s_a) = L_{dec}(c_a) - L_{dem}(x_1^r(\bar{I}_1)). \tag{14}$$

The LLR are further interleaved to produce the extrinsic LLR, $L_{map}(x_1^r)$, of chips x_1^r. This extrinsic LLR is feedback to the MUD to update *a priori* LLR by determining new values for the mean and variance for the next iteration, respectively, and can be expressed as [24]:

$$E(x_1^r) = \tanh(L_{map}(x_1^r)/2),\quad \mathrm{Var}(x_1^r) = 1 - E(x_1^r)^2. \tag{15}$$

Finally, the SISO channel decoder computes *a posteriori* LLR for every information bit L_p, which is used to make a hard decision on the decoded bits at the last iteration to obtain D_p. The final process performs an XOR operation between the original information bits of each users and the output of the decoder to determine the desired information for each user sent by their partner and can be described as

$$\hat{d}_k = D_p \oplus d_{k-1}\,,\quad \hat{d}_{k-1} = D_p \oplus d_k\,. \tag{16}$$

3. ATMOSPHERIC CHANNEL MODEL

The channel state h_k models the optical intensity fluctuations for the TWR-FSO link resulting from the atmospheric loss, turbulence and misalignment-induced channel fading, which can be described as

$$h_k = h_l\,h_s\,h_E\,, \tag{17}$$

where h_l is the channel loss coefficient, h_s is a random variable representing the intensity fluctuation due to atmospheric turbulence, and h_E is the misalignment fading due to the PE loss. The following subsections describe the mathematical expression for each of these.

A. Atmospheric Loss
The atmospheric channel attenuates the signal traversing it as a result of absorption and scattering processes and is described by the exponential Beers-Lambert Law as [27]:

$$h_l = \exp(-\delta\,L), \tag{18}$$

where L is the transmission distance, and δ is the weather attenuation coefficient and it can be determined from the visibility data through Kim's model as

$$\delta = (3.91/V)(\lambda/550)^{-q}\,, \tag{19}$$

where V is the visibility, λ is the wavelength, and q being the particle size distribution coefficient [27].

B. Atmospheric Turbulence-Induced Fading

Turbulence fading is one of the main impairments affecting the operation of FSO communication systems. Classical studies on optical wave propagation have been classified in two major categories, either the weak or strong fluctuations theory. To describe the atmospheric turbulence and its effects on the optical beam propagation, theoretical and experimental studies have been carried out within the research community in order to develop tractable and reliable mathematical models for the irradiance PDF.

1. Log-Normal Turbulence Model

The log-normal distribution is commonly used to model the weak turbulence condition and has been embraced in many calculations for the turbulence channel [28,29]. The distribution of the light intensity fading induced by weak turbulence can be described by log-normal distribution as

$$p(h_s) = \frac{1}{\sqrt{2\pi \sigma_I^2}\, h_s} \exp\left(\frac{\left[\ln(h_s) + \sigma_I^2/2\right]^2}{2\sigma_I^2}\right), \qquad \textbf{(20)}$$

where σ_I^2 is the scintillation index and for a weak turbulence regime is found to be proportional to Rytov variance σ_R^2, which can be calculated as

$$\sigma_R^2 = \hbar C_n^2 \left(2\pi/\lambda\right)^{7/6} L^{11/6}, \qquad \textbf{(21)}$$

where C_n^2 is the refractive index structure parameter, and $\hbar$ is a constant given by

$$\hbar = \begin{cases} 1.23 & \text{for plane wave} \\ 0.5 & \text{for spherical wave} \end{cases}. \qquad \textbf{(22)}$$

A plane wave model is used for starlight and other exo-atmospheric sources while spherical wave model is used for a small- aperture source within or near the turbulent atmosphere.

2. Gamma-Gamma Turbulence Model

The gamma-gamma distribution is a more recent fading model [30], which has evolved from an assumed modulation process, in order to address the large- and small-scale scintillations under moderate-to-strong scenarios. The gamma-gamma PDF is given by

$$p(h_s) = \frac{2(\alpha\beta)^{(\alpha+\beta)/2}}{\Gamma(\alpha)\Gamma(\beta)} h_s^{((\alpha+\beta)/2)-1} K_{\alpha-\beta}\left(2\sqrt{\beta\alpha h_s}\right), \qquad \textbf{(23)}$$

where $\Gamma(.)$ is the Gamma function and $K_{\alpha-\beta}(.)$ denotes the modified Bessel function of the second kind of order $\alpha-\beta$. Parameters α and β represent the effective number of large-scale and small-scale turbulence eddies, respectively, and their values can be calculated according to the expressions provided in [31].

C. Pointing Errors

The misalignment-fading model derived in [32] offers a tractable PDF for describing the behaviour of the PE loss, which takes into account the detector size, beam width and jitter variance. The model assumes a circular detection aperture of radius a, and a

Gaussian spatial intensity profile of beam waist radius w_L on the Rx plane at distance L. The pointing loss is given by [33,34]

$$h_s = A_o \exp(-2r^2/w_{Leq}^2), \qquad \textbf{(24)}$$

where r is the radial displacement between beam centre and centre of the detector, and

$$A_o = \left(\text{erf}(v_p)\right)^2, \quad v_p = \sqrt{\pi/2}(a/w_L). \qquad \textbf{(25)}$$

where A_o is the fraction of the received power at a zero radial distance, erf$(.)$ denotes the error function and w_L/a identifies the beam waist normalized by the radius of the receiver aperture. w_{Leq}^2 represents the equivalent beam waist and can be determined as

$$w_{Leq}^2 = w_L^2 \sqrt{\pi}\, erf(v_p)/2v_p \exp(-v_p^2). \qquad \textbf{(26)}$$

4. BIT-ERROR RATE

For an BPSK IM/DD FSO communication link, the BER defines as $P_e = p(0)p(e|0) + p(1)p(e|1)$, where $p(0)$ and $p(1)$ represent the probabilities of transmitting 0 and 1 bits, respectively, while $p(e|0)$ and $p(e|1)$ resemble the conditional bit error probabilities when the transmitted bit is 0 or 1, respectively. Assuming that the transmitter is sending 1s and 0s with equal probability, each has a probability equalled to 0.5, it is easy to show that BER conditioned on h

$$P_e(e|h_k) = Q\left(\sqrt{\frac{P_t R h_k}{\sigma}}\right), \qquad \textbf{(27)}$$

where $Q(.)$ is the Gaussian Q-function. However, the average BER can be determined by averaging the conditional bit error probabilities over PDF of h_k, which is expressed as [35]

$$P_e = \int_0^h p(h_k)\, P_e(e|h_k)\, dh_k. \qquad \textbf{(28)}$$

For log-normal distribution, substituting Eq. (20) into Eq.(28) and using a Gauss–Hermit quadrature integration, the average BER can be determined as [36]

$$P_e = \frac{1}{\sqrt{\pi}}\sum_{i=0}^{\mathbb{z}} \mathbb{w}_i Q\left[\exp(\sqrt{2}\sigma_R \mathbb{x}_i - \sigma_R^2/2)\right], \qquad \textbf{(29)}$$

where $\mathbb{w}_i$ and $\mathbb{x}_i$ are weight factors and the zeros of an zth order Hermite polynomial, respectively [36]. The channel state distribution for strong turbulence regime is given by [37]

$$p(h) = \frac{2\varsigma^2(\alpha\beta)^{(\alpha+\beta)/2}}{(A_o h_l)^{\varsigma^2}\Gamma(\alpha)\Gamma(\beta)} h^{\varsigma^2-1}$$
$$\times \int_{h/A_o h_l}^{\infty} h_s^{((\alpha+\beta)/2)-1} K_{\alpha-\beta}\left(2\sqrt{\beta\alpha h_s}\right) dh_s, \qquad \textbf{(30)}$$

where $\varsigma = w_{Leq}/2\sigma_s$ is the ratio between the equivalent beam width at the Rx and the PEs standard deviation. For the gamma-gamma distribution model, Eq.(30) can be simplified using Meijer G-function $G_{1,3}^{3,0}$ as [38]

$$p(h) = \frac{(\alpha\beta)\varsigma^2}{A_o h_l \Gamma(\alpha)\Gamma(\beta)} G_{1,3}^{3,0}\left(\frac{\alpha\beta h}{A_o h_l}\middle|\begin{array}{c}\varsigma^2 \\ \varsigma^2-1, \alpha-1, \beta-1\end{array}\right). \qquad \textbf{(31)}$$

Therefore, the average BER can be realized by substituting Eq. (31) into Eq. (28), which gives [22]
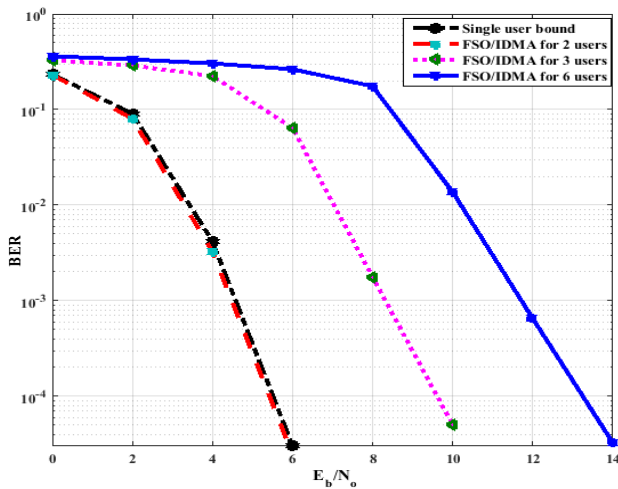
$$P_e = \frac{2^{(\alpha+\beta-4)}\xi^2}{\sqrt{\pi^3}\Gamma(\alpha)\Gamma(\beta)}$$

$$\times G_{7,4}^{2,6}\left(\frac{(A_o h_l)^2}{(\alpha\beta\sigma)^2} \left| \begin{matrix} \frac{1-\xi^2}{2},\frac{2-\xi^2}{2},\frac{1-\alpha}{2},\frac{2-\alpha}{2},\frac{1-\beta}{2},\frac{2-\beta}{2},1 \\ 0,\frac{1}{2},\frac{-\xi^2}{2},\frac{1-\xi^2}{2} \end{matrix} \right. \right). \qquad \textbf{(32)}$$
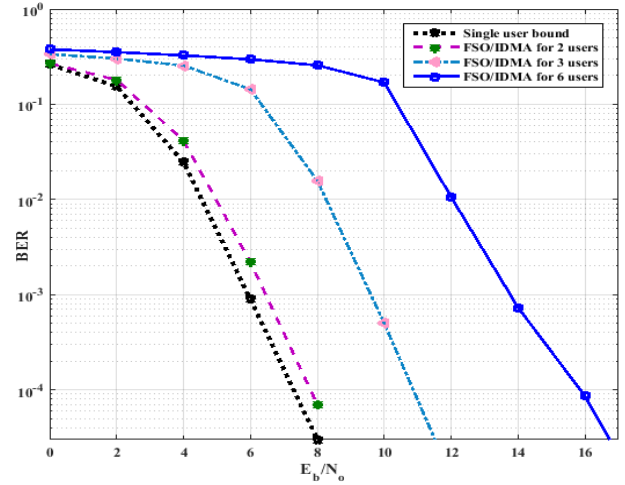
5. NUMERICAL RESULTS AND DISCUSSION

In this section, the performance of the three system models, namely, FSO/IDMA, TWR-FSO PNC and I-MUD FSO PNC, have been evaluated in terms of the BER against the energy-to-noise ratio (E_b/N_o), where E_b is the bit energy, under the influence of the channel impairments such as path loss, atmospheric turbulence and PEs. The strength of the irradiance fluctuation can be determined through the value of Rytov variance σ_R^2. This value assumed to vary between $0.1 \le \sigma_R^2 \le 1$ for weak turbulence and $\sigma_R^2 \gg 1$ for moderate-to-strong turbulence regimes. We considered a TWR- FSO link with $\lambda = 850$ nm, path loss = 0.8 under the clear weather condition at $V = 10$ km with the standard deviation (jitter) of PE displacement $\sigma_s = 0.3$ m, normalized beam width $w_L/a = 25$ and normalized jitter $\sigma_s/a = 3$ [31, 32].

A. FSO/IDMA Model

In communication networks, MA is essential, and several techniques have been widely adopted, which permit multiple users to transmit and receive information at the same time to the base station in a given bandwidth with a given link reliability. Recently, IDMA as a special case of the code-division MA system has gained significant research attention, and it can be considered one of the most promising candidates for the uplink in future wireless communication systems. Moreover, MA techniques were also proposed in FSO based communication networks, and their performance was investigated under the weak, and strong atmospheric turbulence regimes [39,40]. In this paper, this technique is applied for the FSO communication link to allow multiple users to simultaneously share the same resource of atmospheric channels. In this scheme, the K users transmitted to their perspective destinations without the help of the RN.
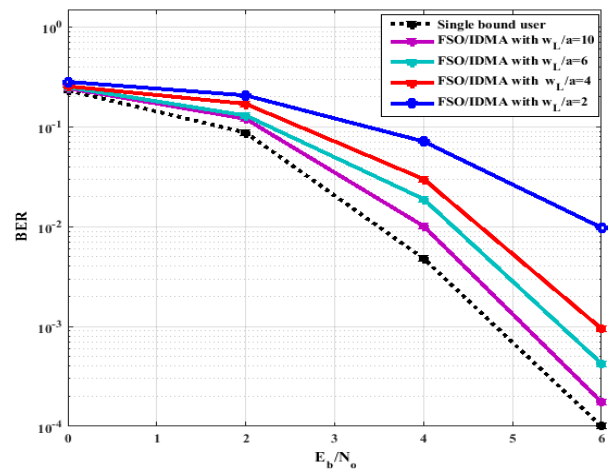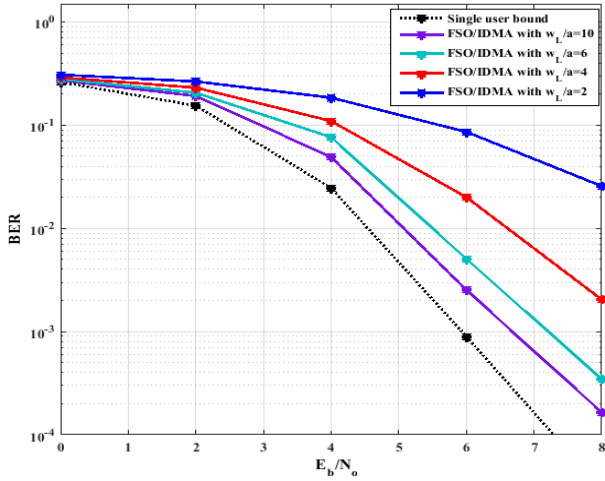

Fig. 6. Simulated BER performance against E_b/N_o for FSO/IDMA system under gamma-gamma distribution with $K = 2,3,6$, $R_c = 1/2$, $R_r = 1/8$, $\lambda = 850$ nm and $L = 1$ km under clear weather condition at $V = 10$ km.

However, investigation of the performance FSO/IDMA system is simulated for different number of simultaneous user $K = 2,3$ and 6 with the convolutional code at a rate $R_c = 1/2$ and the spreading code at a rate $R_r = 1/8$. The simulated BER performances of the system against E_b/N_o over log-normal and gamma-gamma channels are shown in Figs. 5 and 6, respectively. The corresponding single user bound BER performance is also included for reference. In weak turbulence condition, we observed a degradation in the BER performance with respect to E_b/N_o when K increases from 2 to 6 users. For instance, to achieve a BER of 10^{-4}, the E_b/N_o gains are 5.5 and 13.2 dB for $K = 2$ and 6, respectively, under the influence of the atmospheric turbulence channel characterized by σ_R^2. The E_b/N_o penalty is 8.1 dB for $K = 2$ compared to that of $K = 6$ under the strong turbulence condition. These results indicate that the system performance is highly sensitive to the atmospheric turbulence, which requires higher received optical power to overcome the BER degradation. Moreover, the simulated results reveal that the

Fig. 5. Simulated BER performance again E_b/N_o for FSO/IDMA system under weak turbulence conditions at $L = 1$ km under clear weather condition at $V = 10$ km and $K = 2,3,6$.

Fig. 7. Simulated BER performance against E_b/N_o of the FSO/IDMA system for different numbers of normalized beam width w_L/a with fixed normalized jitter at $\sigma_s/a = 3$ applying log-normal distribution.
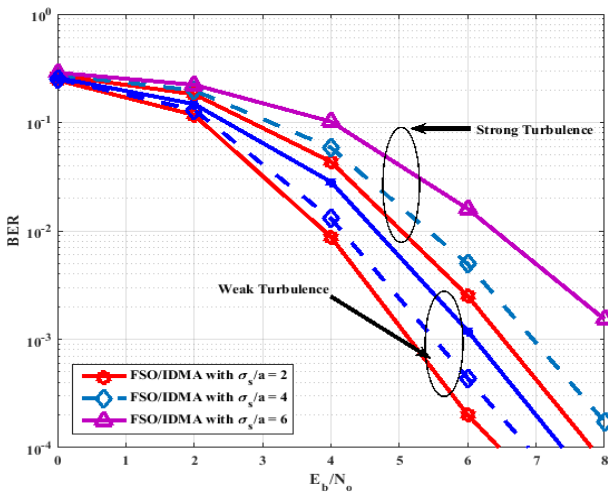
Fig. 8. Simulated BER performance against E_b/N_o for FSO/IDMA system for different numbers of normalized beam width w_L/a with fixed normalized jitter at $\sigma_s/a = 3$ under strong turbulence.

BER performance is limited mainly by the MAI, which arises when there are number of users in the system.

Additionally, scintillation affects the laser beam propagation and ultimately causes fluctuation of the received signal. Thus, the information encoded in the intensity of the carrier signal is much more prone to these impairments. Accordingly, for higher values of K, E_b/N_o penalties are higher for weak and strong turbulence regimes. Subsequently, the system is unable to guarantee a reliable communication service for the entire turbulence strength regimes. Therefore, for $K = 2$ the simulated BER performance of the FSO/IDMA system is closer to the single user bound performance. To illustrate the effect of PEs on the performance of FSO/IDMA system, the influence of the beam width and jitter are considered. Figures 7 and 8 depict the simulated BER performance against E_b/N_o under weak and strong turbulence regimes for a range of normalized beam width $w_L/a = 2,4,6$ and 10 with a fixed normalized jitter $\sigma_s/a = 3$, respectively.

Fig. 9. Simulated BER performance against E_b/N_o for FSO/IDMA system for different numbers of normalized jitter σ_s/a and fixed normalized beam width $w_L/a = 10$ under weak and strong turbulence.

Figure 9 displays the simulated BER performance against E_b/N_o under weak and strong turbulence condition for a range of normalized jitter $\sigma_s/a = 2,4$ and 6 with a fixed normalized beam width $w_L/a = 10$. The figures reveal that in FSO/IDMA widening the beam width can mitigate the effect of PEs, thus resulting in the BER performance approaching that of the single user bound. Meanwhile, narrowing the beam width will contribute to the problem of misalignment and beam wandering. As observed also, the system performance decreases when σ_s/a decreases. Therefore, the transceiver design with an optimum value of the beam width for higher values of normalized jitter in order to increase the robustness of the link in the presence of PEs was considered [35].

B. TWR-FSO PNC model

As the only essential requirement for an FSO system is the need for the line-of-sight (LOS) path between Tx and Rx, the relay-assisted FSO solution can be effectively used to establish communications between FSO nodes located over longer link distances. However, an FSO link severely suffers from strong turbulence and is far away from satisfying the typical BER targets for FSO applications within the practical ranges of E_b/N_o. Therefore, to combat fading and maintain acceptable performance levels, the relay-FSO technique is used by taking advantage of a shorter link or multiple hops between Tx and Rx. However, the TWR-FSO PNC scheme is adopted here to broaden the signal coverage for a given limited transmit power and mitigate fading over long transmission span (i.e., > 1 km). This model allows the two FSO nodes to exchange their information through a single RN with minimum transmission phases (MA and BC). This results in improved spectral efficiency, which in turn boosts the network throughput. The performance of the TWR-FSO PNC system for two users (i.e., $K = 2$) is evaluated by means of simulation for atmospheric turbulence with log-normal and gamma-gamma distributions. The simulations are run under the clear weather condition for $V = 10$ km, $L = 2$ km and $\lambda = 850$ nm.

Figure 10 presents the predicted BER performance for a FSO link between Tx and Rx using Eqs. (29) and (32) for weak and strong turbulence conditions, respectively, and the simulated BER performance of TWR-FSO PNC in terms of E_b/N_o for a range of Rytov variance. In this model, the end-to-end link in TWR-FSO PNC was considered, where the RN performed PNC demapping on the superimposed received signal, which reduces the system complexity but at the cost of performance degradation at the destination nodes due to un-corrected errors at the RN. However, it was observed from the preliminary results that at higher E_b/N_o (i.e., ≥ 8 dB) the performance of the TWR-FSO PNC model had a slightly worse BER performance then the predicted BER for higher turbulence levels. For example, at a BER of 10^{-4} and for $\sigma_R^2 = 0.5$ an additional E_b/N_o of ~7dB is required compared to the case with $\sigma_R^2 = 0.2$. Moreover, it is worth stating that an end-to-end BER of TWR-FSO PNC was evaluated for two transmission phases in which the system will experience channel fading. This is caused by fluctuation of the signal strength while propagating over a communication channel that had a significant effect on performance of the system. Whereas the LOS FSO system consists of a single hop transmission phase. For example, to achieve a BER of 10^{-4} with a fading strength of $\sigma_R^2 = 0.5$, a E_b/N_o gain of about 29 dB is required for the predict FSO system. whereas, to obtain the same BER for TWR-FSO PNC, 30 dB of E_b/N_o gain is required.

The severity of the small-scale fading in the optical wireless channel is distance-dependent; therefore, in TWR-FSO to combat
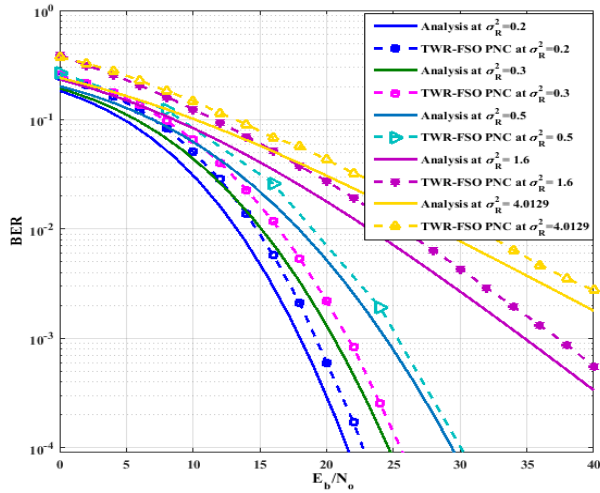
Fig. 10. Predict and simulated BER performance against E_b/N_o for TWR-FSO PNC system at $K = 2$ km, $\lambda = 850$ nm and $L = 2$ km under clear weather condition at $V = 10$ over weak- moderate - strong turbulence conditions.

fading one needs to reduce the distance between the Tx and the Rx. Figure 11 presents the simulated BER performance for the TWR-FSO PNC system in terms of E_b/N_o under the weak and strong atmospheric turbulence regimes for a range of transmission spans $L = 2,6,12$. It can be observed that at a BER of 10^{-4} and for $L = 12$ km, λ of 850 nm higher E_b/N_o values of 34 dB and 57 dB are required for weak and moderate turbulence regimes, respectively. While for the same BER and $L = 6$ km, lower values of E_b/N_o about 27 dB and 52 dB are attained for the weak and moderate turbulence regimes, respectively. This is expected, since optical beams are less susceptible to the attenuation caused by absorption and scattering for a shorter propagation link. Whereas, optical beams propagating over longer link distances (i.e., > 1 km) will experience higher attenuation due to absorption caused by the presence of atmospheric particles.
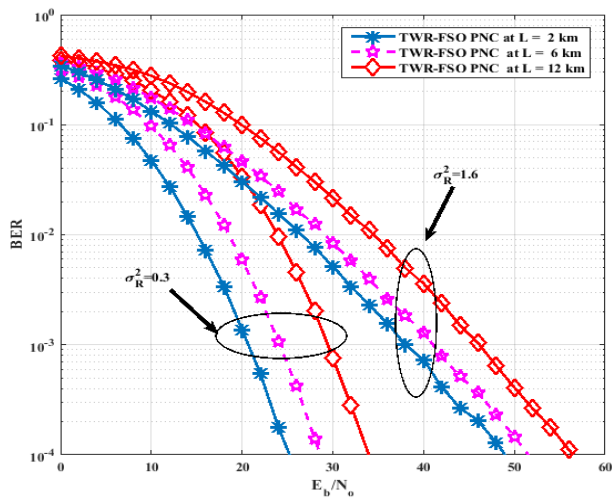
However, the advantage of the TWR-FSO PNC is to reduce the complexity at the RN by performing a specialist detected-and-forward scheme in order to map the signal at the RN. This is in contrast to other traditional relay-assisted FSO system, which employs AF and DF strategies to process the signal at the intermediate node. In addition, TWR-FSO PNC increases the network throughput by reducing the transmission phases that are required to complete data exchange between two users.

C. I-MUD FSO Based PNC

A MUD technique is necessary to separate different users' signals that share the same propagation media and improve the performance by jointly processing signals from all users. Thus, numerous suboptimal MUDs have been considered to mitigate interference with respect to the system performance, complexity, and the requirements with regard to the channel state information. In turbo processor, each decoder handles the data for a certain user only and disregards the others. Therefore, complexity of the decoder is independent of K. Hence, TWR-FSO PNC model is extended to allow multiple users exchanging information via a single RN over the FSO link when there is no direct link between them, as shown in Fig. 1. In this section, the performance of I-MUD TWR-FSO PNC model is investigated. The simulated BER performance for the proposed system in terms of E_b/N_o for a given number of users $K = 4,12$ and 20 under the weak atmospheric turbulence regime, and considering the path loss and PEs at $\lambda = 850$ nm under the clear weather condition at $V = 10$ km and $L = 2$ km (where the distance between a user and relay is 1 Km) is presented in Fig. 12. The simulation result shows that there is an improvement in the BER performance for the I-MUD FSO PNC model compared to TWR-FSO PNC despite the increased number of simultaneous users. For instance, at a BER of 10^{-4}, the E_b/N_o gains are ~14, 10 and 7 dB for I-MUD FSO PNC with respect to TWR-FSO PNC. Furthermore, the simulated BER performance for the system under consideration in terms of E_b/N_o is evaluated under strong turbulence for $\lambda = 850$ nm and $L = 2$ km under the clear condition at $V = 10$ km for a number of users $K = 4, 8$ and 14, as shown in Fig. 13. Although the number of the concurrent users is increasing, the proposed

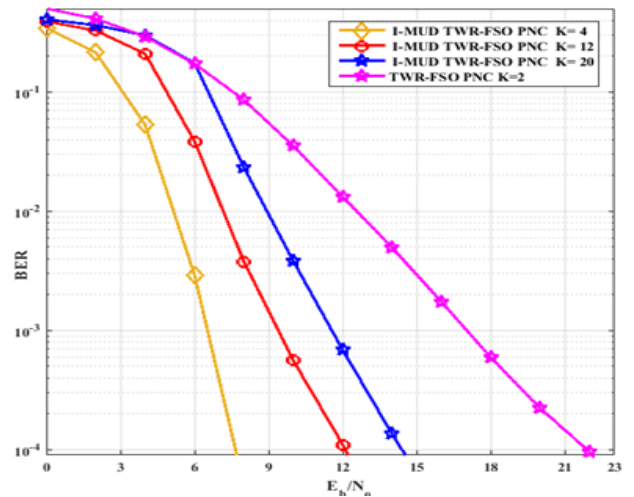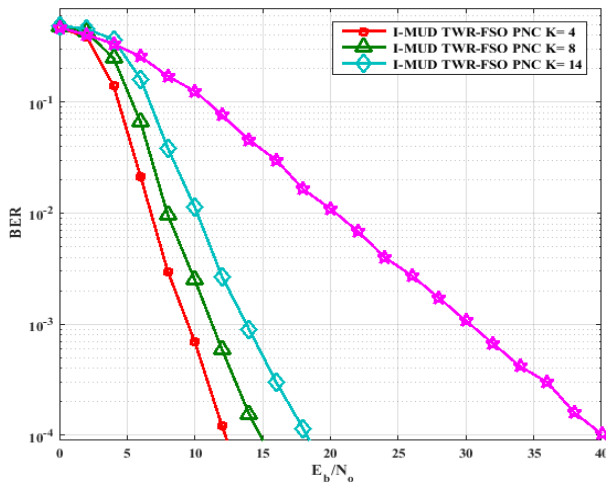**Fig. 11.** Simulated BER performance against E_b/N_o for TWR-FSO PNC system under weak and strong turbulence regimes for $L = 2,6,12$ km, $\lambda = 850$ nm under the clear weather condition at $V = 10$ km.

Fig. 12. Simulated BER performance against E_b/N_o for TWR-FSO PNC and I-MUD FSO based PNC systems under weak turbulence for $K = 2,4,12,20$, $\lambda = 850$ nm and $L = 2$ km under the clear weather condition at $V = 10$ km.

Fig. 13. Simulated BER performance against E_b/N_o for TWR-FSO PNC and I-MUD FSO based PNC under strong turbulence for $K = 2,4,8,14$, $\lambda = 850$ nm and $L = 2$ km under the clear weather condition at $V = 10$ km.

system offers improved BER performance. For example, at a BER of 10^{-4}, the E_b/N_o gains are 28, 25 and 22 dB with respect to TWR-FSO PNC. It can be explained that by iteratively updating the transmitted symbol pair probabilities, the MUD produces more accurate *a priori* probabilities of the XOR-ed coded bits for the DECs, which can enhance the system performance. Additionally, an alternative mitigation scheme known as aperture averaging can be adopted in order to achieve improvement in the BER performance under turbulence-induced scintillation and PE conditions.

6. CONCLUSIONS

Physical layer network coding is a promising technique that has great potential for improving the achievable data rates of end-to-end flows through higher data transmission rates, thereby increasing the overall network throughput. We studied the performance of the TWR-FSO PNC transmission technique for FSO wireless networks when there is no direct path between the two communication nodes. The system was simulated for attainable BER performance by transmitting BPSK symbols over the weak and strong atmospheric turbulence fading channels, taking into account the other physical layer impairments including atmospheric attenuation and PE. In this paper, to allow multiple users to simultaneously share the same resources of FSO link, an IDMA technique was applied. We investigated the BER performance of the FSO/IDMA system over log-normal and gamma-gamma models. The result showed that there was E_b/N_o penalty of ~9 dB at a BER of 10^{-4} under strong turbulence for $K = 6$ with respect to single user bound resulting from the MAI and scintillation effects. Consequently, the simulation for the I-MUD FSO based PNC model was carried out, where multiple nodes could exchange information through a single relay over a FSO link when there is no direct link between them. The TWR-FSO technique was adopted to alleviate the influence of the scintillation by reducing the transmission range and increasing spectral efficiency. Additionally, the effect of I-MUD algorithm and chip-interleaving was considered to mitigate MAI. Simulation results showed an improved BER performance even for higher number of simultaneous users. For instance, new model offered

~8 and 22 dB of E_b/N_o gains to achieve a BER of 10^{-4} for $K = 20,14$ with respect to TWR-FSO PNC under weak and strong turbulence regimes, respectively.

REFERENCES

1. S. S. Muhammad, T. Plank, E. Leitgeb, A. Friedl, K. Zettl, T. Javornik, and N. Schmitt, "Challenges in establishing free space optical communications between flying vehicles," *6th International Symp. Commun. Syst. Net. Digital Signal Proc. Conf.* (CNSDSP), pp. 82-86 (2008).
2. T. Xuan, W. Zhaocheng, X. Zhengyuan, and Z. Ghassemlooy, "Multihop free-space optical communications over turbulence channels with pointing errors using heterodyne detection," *Journal of Lightwave Technology,* vol. 32, pp. 2597-2604, (2014).
3. J. Libich, M. Komanec, S. Zvanovec, P. Pesek, W. O. Popoola and Z. Ghassemlooy, "Experimental verification of an all-optical dual-hop 10 Gbit/s free-space optics link under turbulence regimes," *Optics letters,* vol. 40, no. 3, pp. 391-394, (2015).
4. E. Zedini and M. S. Alouini, "On the Performance of Multihop Heterodyne FSO Systems with Pointing Errors*," IEEE Photonics Journal,* vol. 7, no. 2, pp. 1-10, (2015).
5. M. Safari, M. Uysal, "Relay-assisted free-space optical communications", *IEEE Trans. Wireless Commun.* 7, pp. 5441–5449 (2008).
6. A. Sendonaris, E. Erkip, and B. Aazhang, "User cooperation diversity: Part I. System description," *IEEE Trans. Commun.* 51, pp. 1927–1938 (2003).
7. R. Ahlswede, N. Cai, S. Y. R. Li, and R. W. Yeung, "Network information flow," *IEEE Trans. Information Theory* 46, pp. 1204-1216 (2000).
8. K. Minkyu, M. Medard, and U. M. O'Reilly, "Network coding and its implications on optical networking," *Opt. Fiber Commun. Conf.* (*OFC*) pp. 1-3 (2009).
9. A. E. Kamal,"1+N network protection for mesh networks: network coding-based protection using p-Cycles," *IEEE/ACM Trans. Net.*18, pp. 67-80 (2010).
10. E. D. Manley, J. S. Deogun, L. Xu, and D. R. Alexander, "All-Optical network coding," J. *Opt. Commun. Net.* 2, pp. 175-191 (2010).
11. X. Zhou, D.I. Zhang, Y. Yang and M.S. Obaidat, "Network-coded multiple-source cooperation aided relaying for free-space optical transmission", *International J. Commun. Syst. pp.* 1465–1478 (2012).
12. Y. Tang, X. Zhou, Z. Zhang, and Q. Tian, "Performance analysis of a two-way network-coded free space optical relay scheme over strong turbulence channels," *IEEE in Vehicular Technology Conference (VTC),* pp. 1-5 (2011).
13. P. Puri, P. Garg, M. Aggarwal, and P. K. Sharma, "Outage analysis of two-way relay assisted FSO systems over weak turbulence region," *Annual IEEE in India Conference (INDICON)*, pp. 1-5 (2013).
14. P. Puri, P. Garg, and M. Aggarwal, "Outage and error rate analysis of network coded coherent TWR-FSO systems," *Photonics Technology Letters, IEEE*, vol. 26, pp. 1797-1800 (2014).
15. S. L. Zhang, S. C. Liew, and P. P. Lam, "Hot Topic: Physical-layer network coding," *Mobicom*, pp. 358-365 (2006).
16. Z. Abu-Almaalie, Z. Ghassemlooy, H. Le-Minh, and N. Aslam, "Physical layer network coding with two-way relay free space optical communication link," *Internet Tech. Applications* (ITA), pp. 292-297 (2015).
17. S. Shukla, V. T. Muralidharan, and B. S. Rajan, "Wireless network-coded three-way relaying using Latin cubes*," 23rd International Symp. Personal Indoor and Mobile Radio Commun.* (PIMRC), pp. 197-203 (2012).
18. S. Shukla and B. S. Rajan, "Wireless network-coded four-way relaying using Latin Hyper-Cubes," *Wireless Commun. Net. Conf.* (WCNC) pp. 2410-2415 (2013).
19. C. Min and A. Yener, "Multiuser two-way relaying for interference limited systems," *International Commun. Conf.* (ICC), pp. 3883-3887 (2008).

20. Z. Abu-Almaalie, Z. Ghassemlooy, H. Le-Minh, and N. Aslam, "Performance evaluation of IDMA implementation with physical layer network coding," *9th International Symp. Commun. Syst. Net. Digital Signal Proc.* (CSNDSP), pp. 700-705 (2014).
21. F. Lenkeit, C. Bockelmann, D. Wubben, and A. Dekorsy, "IRA code design for IDMA-based multi-pair bidirectional relaying systems," *IEEE Globecom Workshops* (GC Wkshps), pp. 241-246 (2013).
22. K. Prabua, D. S. Kumara, R. Malekianb, "BER analysis of BPSK-SIM based SISO and MIMO FSO systems in strong turbulence with pointing errors," *International J. Light Elect. Opt.* 125, pp. 6413-6417 (2014).
23. P. Li, L. Lihai, W. Keying, and W. K. Leung, "Interleave division multiple-access," *IEEE Trans. Wireless* Commun. 5, pp. 938-947 (2006).
24. S. Rajbhandari, Z. Ghassemlooy, P. A. Haigh, T. Kanesan, and Xuan Tang, "Experimental error performance of modulation schemes under a controlled laboratory turbulence FSO channel," *J. Lightwave Tech.* 33 .1, pp. 244-250 (2015).
25. F. Dong, L. Peng, A. Burr, and R. de Lamare, "Physical-layer network coding based interference exploitation strategy for multi-user hierarchical wireless networks," *18th Europe. Wireless Conf.,* pp. 1-6 (2012).
26. H. Yi and L. K. Rasmussen, "Iterative switched decoding for interleave-division multiple-access systems," *IEEE Trans. on Vehicular Tech.* 57, pp. 1939-1944 (2008).
27. I. Kim, B. McArthur, and E. Korevaar, "Comparison of laser beam propagation at 785 nm and 1550 nm in fog and haze for optical wireless communications," *in Proc. SPIE, Optical Wireless Communications III*, pp. 26-37, 2001.
28. L.C. Andrews and R.L, Philips, *laser beam propagation through random media*, (2005).
29. Z. Xiaoming and J. M. Kahn, "Free-space optical communication through atmospheric turbulence channels," *IEEE Trans. Commun.* 50, pp. 1293-1300 (2002).
30. S. Xuegui, Y. Fan, and C. Julian, "Subcarrier BPSK modulated FSO communications with pointing errors*," IEEE Wireless Commun. Net. Conf. (WCNC),* pp. 4261-4265 (2013).
31. Z.Ghassemlooy, W. O. Popoola, and E. Leitgeb, "Free-space optical communication using subcarrier modulation in gamma-gamma atmospheric turbulence," 9th *International Transp. Opt. Net. Conf.* (ICTON), pp. 156-160 (2007).
32. A. A. Farid and S. Hranilovic, "Outage capacity optimization for free-space optical links with pointing errors," *J. Lightwave Tech.* 25, pp. 1702-1710 (2007).
33. H. L.-Q. W. Zhibin, "A Closed-form expression for BER of FSO links over gamma-gamma atmospheric turbulence channels with pointing errors," *J. Applied Sciences, Eng. Tech.* 6, pp. 1272-1275 (2013).
34. J. Park, E. Lee, C. B. Chae and G. Yoon, "Impact of pointing errors on the performance of coherent free-space optical systems," *Phot. Tech. Lett.* 28. 2, pp. 181-184 (2016).
35. A. K. Majumdar*, Advanced Free Space Optics (FSO): A Systems Approach,* vol. 186, 2014.
36. W. O. Popoola, Z. Ghassemlooy, J. I. H. Allen, E. Leitgeb, and S. Gao, "Free-space optical communication employing subcarrier modulation and spatial diversity in atmospheric turbulence channel," *IET Optoelectronics*, vol. 2, pp. 16-23, (2008).
37. I. E. Lee, Z. Ghassemlooy, W. P. Ng, and M. Uysal, "Performance analysis of free space optical links over turbulence and misalignment induced fading channels," 8th International Symp. Commun. Syst. Net. Digital Signal Proc. (CSNDSP), pp. 1-6 (2012).
38. C. Zhang, Si, Y. Wang Y., J. Wang and J. Jia," Average capacity for non-Kolmogorov turbulent slant optical links with beam wander corrected and pointing errors," *International Journal for Light and Electron Optics*, vol. 123, no.1, pp.1-5, (2012).
39. N. T. Dang, H. T. T. Pham, and A. T. Pham, "Reducing atmospheric turbulence effects in FSO/CDMA systems by using multi-wavelength PPM signaling," *18th Asia-Pacific Commun. Conf.* (APCC), pp. 338-343 (2012).
40. F. Jingyuan, Z. Xiaolin, and L. Jun, "Design and evaluation of an IDMA cooperative relay free-space optical system," *International Space Opt. Syst. Applications Conf.* (ICSOS), pp. 358-362 (2011).